DOI: 10.1002/ejic.201100032

# Synthesis and Crystal Structures of μ-Oxido- and μ-Hydroxido-Bridged Dinuclear Iron(III) Complexes with an $N_2O$ Donor Ligand – A Theoretical Study on the Influence of Weak Forces on the Fe–O–Fe Bridging Angle

**Rituparna Biswas,[a] Michael G. B. Drew,[b] Carolina Estarellas,[c] Antonio Frontera,*[c] and Ashutosh Ghosh*[a]**

**Keywords:** Iron / Schiff bases / N,N,O ligands / Crystal structures / Density functional calculations

The synthesis and crystal structures of three nonheme di-iron(III) complexes with a tridentate N,N,O Schiff-base ligand, 2-({[2-(dimethylamino)ethyl]imino}methyl)phenol (HL), are reported. Complexes $[Fe_2OL_2(NCO)_2]$ (**1a**) and $[Fe_2OL_2(SAL)_2]\cdot H_2O$ [SAL = *o*-$(CHO)C_6H_4O^-$] (**1b**) are unsupported μ-oxido-bridged dimers, and $[Fe_2(OH)L_2(HCOO)_2(Cl)]$ (**2**) is a μ-hydroxido-bridged dimer supported by a formato bridging ligand. All complexes have been characterized by X-ray crystallography and spectroscopic analysis. Complex **1b** has been reported previously; however, it has been reinvestigated to confirm the presence of a crucial water molecule in the solid state. Structural analyses show that in **1a** the iron atoms are pentacoordinate with a bent Fe–O–Fe angle [142.7(2)°], whereas in **2** the metal centers are hexacoordinate with a normal Fe–OH–Fe bridging angle [137.9(2)°]. The Fe–O–Fe angles in complexes **1a** and **1b** differ significantly to those usually shown by (μ-oxido)$Fe^{III}$ complexes. A theoretical study has been performed in order to rationalize this deviation. Moreover, the influence of the water molecule observed in the solid-state structure of **1b** on the Fe–O–Fe angle is also analyzed theoretically.

## Introduction

The Fe–O–Fe (μ-oxido)diiron unit is a common structural feature in $Fe^{III}$ compounds.[1] Such compounds are studied extensively mainly because of their relevance as model complexes for metalloenzymes or as intermediates in the catalytic cycles of metalloenzymes. It is well known that in oxido-bridged hemes[2] and Schiff-base complexes of the type $[Fe(salen)]_2X_2$ [salen = 1,2-bis(salicylideneaminato)ethane] $Fe^{III}$ exists exclusively as a pentacoordinate species with antiferromagnetically coupled high-spin $Fe^{III}$ ions.[3] Most of the structurally characterized μ-oxido-bridged di-iron compounds are either in unsupported conditions, i.e. in the absence of other bridges, such as $Fe^{III}$–porphyrins,[4–8] Schiff-base $Fe^{III}$–salen,[3a,9–11] and related compounds[11] or supported by carboxylato and other bridging ligands. Conversely, the hydroxido bridge is relatively unusual.[12] A fundamental structural component of the chemistry of these functional $Fe^{III}$ complexes is the variable Fe–O–Fe bridging angle, which is usually in the range 139–180°. However, in the majority of complexes where other bridging ligands are not present, the angle is close to 180°.[13] The angle is obviously smaller (119–135°) in complexes where a carboxylato bridge supports the oxido bridge.[14] We have used tridentate, $N_2O$ donor Schiff-base ligands extensively to synthesize both discrete and infinite polynuclear complexes of $Cu^{II}$ and $Ni^{II}$ with interesting structures and magnetic properties.[15] $Fe^{III}$ complexes with such ligands are scarce,[16–22] although numerous examples have been reported with salen-type $N_2O_2$ donor ligands.

Herein we report the synthesis and crystal structures of two new dinuclear $Fe^{III}$ complexes, $[Fe_2OL_2(NCO)_2]$ (**1a**) and $[Fe_2(OH)L_2(HCOO)_2(Cl)]$ (**2**), which are obtained when the tridentate Schiff base 2-({[2-(dimethylamino)ethyl]imino}methyl)phenol (HL) reacts with a methanol solution of $FeCl_3$ in the presence of an anionic coligand, cyanato (for **1a**) or formato (for **2**). The same ligand has already been used to synthesize $[Fe_2OL_2(SAL)_2]\cdot H_2O$ [SAL = *o*-$(CHO)C_6H_4O^-$] (**1b**).[23] We have repeated the synthesis and crystal structure determination of **1b** in order to confirm the presence of a water molecule interacting with the ligand. This water molecule is crucial in the crystal packing as it influences the Fe–O–Fe angle. Curiously, the structures of the three species (**1a**, **1b**, and **2**) are quite different despite the fact that the ligand is the same and all are prepared under similar conditions. Complexes **1a** and **1b** are unsupported oxido-bridged dimers with very different Fe–O–Fe angles, whereas compound **2** is a hydroxido-bridged dimer supported by a formato bridge (see Scheme 1 and Figure 1). Considering the fact that Fe–O–Fe angles vary widely in

[a] Department of Chemistry, University College of Science, University of Calcutta,
92 A. P. C. Road, Kolkata 700009, India
[b] School of Chemistry, The University of Reading,
P. O. Box 224, Whiteknights, Reading RG6 6AD, UK
[c] Departament de Química, Universitat de les Illes Balears,
Crta. de Valldemossa km 7.5, 07122 Palma (Baleares), Spain
Supporting information for this article is available on the WWW under http://dx.doi.org/10.1002/ejic.201100032.

  

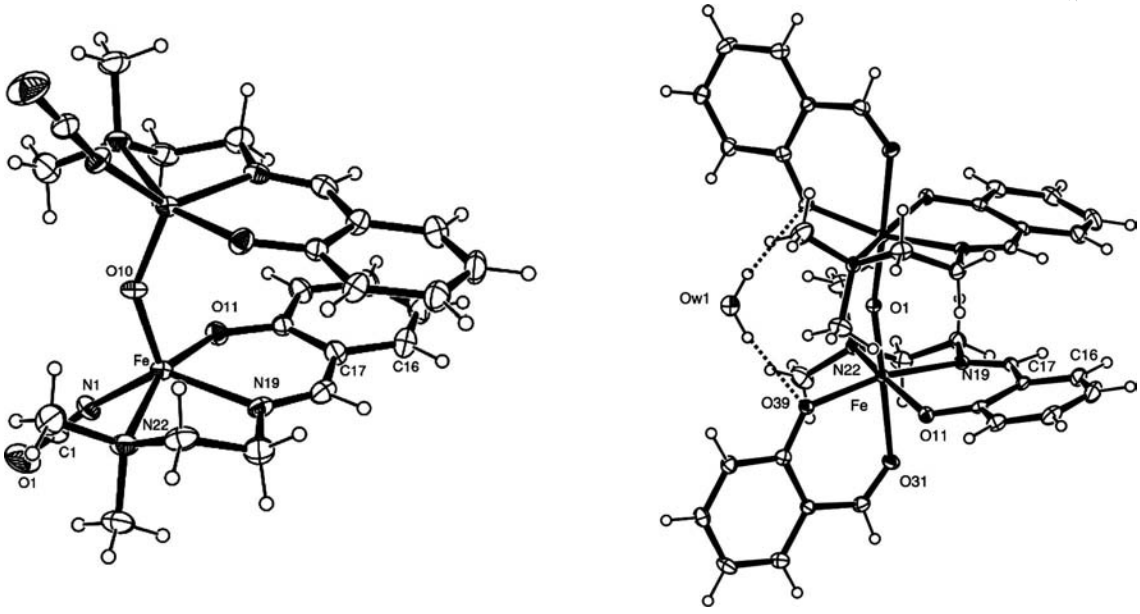


Figure 1. Dimeric structures of **1a** (left) and **1b** (right), which contain crystallographic $C_2$ symmetry. Ellipsoids are plotted at 30% probability.

unsupported oxido-bridged complexes and no theoretical study has been made to rationalize this variation, we have computed the energy profiles of **1a** and **1b** by changing the μ-oxido-bridging angle using DFT calculations. We show here that the difference in energy due to bending is not very high, and weak forces, such as π–π interactions or hydrogen bonds, can dictate the existence of a particular structure in the solid state by compensating for the difference in energy. Therefore, the flexibility of the Fe–O–Fe motif allows the complexes to adopt the most favorable conformation in order to maximize the stabilization provided by weak noncovalent interactions.

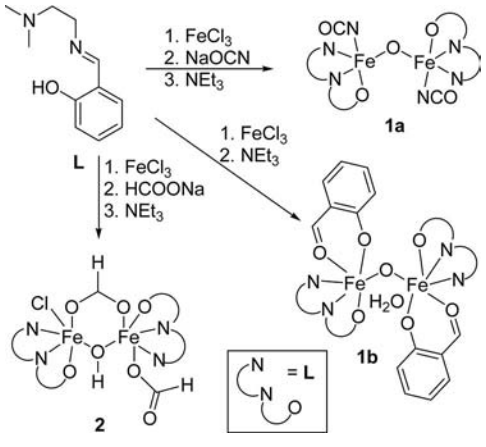


Scheme 1. Synthetic route to **1a**, **1b**, and **2**.

## Result and Discussion

### Synthesis of Compounds

The tridentate Schiff-base ligand was synthesized by condensation of salicylaldehyde and *N*,*N*-dimethylethane-1,2-diamine in a 1:1 molar ratio. $FeCl_3$ reacted with the Schiff-base ligand in a 1:1 molar ratio, and sodium cyanate was added to the reaction mixture resulting in the formation of the dinuclear oxido-bridged iron(III) complex **1a**. Similarly, complex **1b** was synthesized by the reaction of $FeCl_3$ and the Schiff-base ligand in a 1:1 ratio. Complex **2** was obtained by the reaction of $FeCl_3$, the Schiff-base ligand, and sodium formate in a 1:1:2 molar ratio. It is interesting to note that during the formation of **1b**, half of the Schiff-base ligand undergoes hydrolysis, whereas the ligand remains intact in the synthesis of **1a** and **2** although the same conditions were used throughout. We examined the nature of the solid crystalline products for all three compounds, and no visible difference in the nature of the crystalline state was observed indicating that the solids are not mixtures of different compounds. The results of elemental analyses also confirm that the compositions of all three compounds are the same as those determined by X-ray analysis.

### FTIR and UV/Vis Spectra of Complexes

The moderately strong and sharp bands at 1614, 1617, and 1632 $cm^{-1}$ for **1a**, **1b**, and **2**, respectively, are assigned to the ν(C=N) azomethine group. Complex **1a** shows a strong absorption band at 2205 $cm^{-1}$ corroborating the presence of an N-bonded cyanate group. Complex **1b** shows a strong, broad band, centered at 3424 $cm^{-1}$ due to the presence of a water molecule. In complex **2**, strong bands at 1581 and 1448 $cm^{-1}$ are likely to be due to the antisymmetric and symmetric stretching modes for the carboxylate (formate) group, respectively. The formulation of **2** as a hydroxido-bridged compound is also supported by the presence of an O–H stretching band at 3431 $cm^{-1}$. Moreover, two weak absorption bands are observed at 844 and 843 $cm^{-1}$ for **1a**

  

and **1b**, respectively. It is well known that the antisymmetric stretching mode ($\nu_3$), $\nu_{as}$(Fe–O–Fe), of a linear or bent Fe–O–Fe system usually occurs in the 900–800 $cm^{-1}$ region.[24] Thus, these two bands indicate the existence of an Fe–O–Fe linkage in both compounds. The FTIR spectra of **1a**, **1b**, and **2** are shown in Figures S1, S2, S3 (see Supporting Information).

The electronic absorption spectra of the three complexes are similar (see Figures S4a, S4b; S5a, S5b; S6a and S6b in the Supporting Information). The band positions and intensities are comparable with those found in similar complexes.[23,25] The spectra show a strong band with a hump (415, 493 nm for **1a**; 427, 509 nm for **1b**; 411, 510 nm for **2**) assigned to oxido-to-Fe charge transfer (CT). Moreover a moderately strong band (317 nm for **1a**; 318 nm for **1b**; 320 nm for **2**) is tentatively assigned to amino-to-Fe CT. The highest energy bands (255, 231 nm for **1a**; 260, 233 nm for **1b**; 256 and 234 nm for **2**) are attributed to $\pi\rightarrow\pi^*$ transitions of the ligand, but contributions from less intense oxido-to-Fe CT are also expected in this region.[12]

### Description of Crystal Structures of 1a and 2

The structure of **1a** with $C_2$ symmetry, is shown in Figure 1 together with the atom numbering scheme in the metal coordination sphere. Selected bond lengths and angles are summarized in Table 1. Complex **1a** crystallizes in the orthorhombic space group *Fdd*2. The iron atoms are pentacoordinate, bound to three atoms of the tridentate ligand, a nitrogen atom N(1) of an NCO group, and a bridging oxygen atom O(10) positioned at the twofold axis. The geometry of the coordination sphere is best considered as a highly distorted square pyramid with O(10) as the axial atom. The basal plane consists of one oxygen and two nitrogen atoms of the ligand [O(11), N(19), N(22)] and one nitrogen atom [N(1)] of the terminally coordinated NCO group. The four donor atoms in the basal plane show a tetrahedral distortion with deviations of –0.205(2), 0.221(2), –0.238(2), and 0.222(2) Å for N(1), O(11), N(19), and N(22), respectively. The iron atom is 0.515(2) Å from this plane in the direction of the axial O(10) atom. The Fe–O(10) bond length is 1.763(1) Å, which is in the range found for other (μ-oxido)diiron complexes (1.75–1.80 Å). However, unlike other similar oxido-bridged dinuclear iron(III) complexes, the Fe–O–Fe bond angle [142.7(2)°] in **1a** deviates significantly from 180°.[13] The intermetallic Fe–Fe separation is 3.342(1) Å. Bond lengths in the basal plane comprising the $N_2O_2$ donor set are Fe–O(11) 1.926(3) Å, Fe–N(1) 1.958(3) Å, Fe–N(19) 2.108(4) Å, and Fe–N(22) 2.203(3) Å, indicating that the Fe–N distances are significantly longer than the Fe–O bond lengths found in similar complexes of mixed N–O donor ligands, which may result from the greater affinity of iron for oxygen rather than nitrogen.[26] The two phenyl rings on either side of the twofold axis overlap partially at the C(16)–C(17) bonds. The distance between the two bonds (centroid to centroid) is 3.338 Å, which is similar to the π–π stacking distance observed experimentally in organic crystals (3.3–3.6 Å).[27] This issue is discussed further in our theoretical study.

Table 1. Distances [Å] and angles [°] in the metal coordination sphere for **1a** and **2**.

| | | | |
|---|---|---|---|
| **1a** | | | |
| Fe–O(10) | 1.763(1) | O(10)–Fe–N(19) | 109.32(12) |
| Fe–O(11) | 1.926(3) | O(11)–Fe–N(19) | 86.17(12) |
| Fe–N(1) | 1.958(3) | N(1)–Fe–N(19) | 136.88(13) |
| Fe–N(19) | 2.108(4) | O(10)–Fe–N(22) | 93.89(10) |
| Fe–N(22) | 2.203(3) | O(11)–Fe–N(22) | 159.97(12) |
| O(10)–Fe–O(11) | 102.11(11) | N(1)–Fe–N(22) | 89.51(14) |
| O(10)–Fe–N(1) | 112.39(14) | N(19)–Fe–N(22) | 77.14(14) |
| O(11)–Fe–N(1) | 95.35(11) | | |
| **2** | | | |
| Fe(1)–O(31) | 1.913(3) | Fe(2)–O(11) | 1.893(3) |
| Fe(1)–O(10) | 1.934(3) | Fe(2)–O(10) | 1.926(3) |
| Fe(1)–O(4) | 2.013(3) | Fe(2)–O(3) | 2.081(3) |
| Fe(1)–O(1) | 2.018(3) | Fe(2)–N(19) | 2.100(4) |
| Fe(1)–N(39) | 2.116(4) | Fe(2)–N(22) | 2.269(4) |
| Fe(1)–N(42) | 2.274(4) | Fe(2)–Cl(1) | 2.368(2) |
| O(4)–Fe(1)–O(10) | 98.98(13) | O(11)–Fe(2)–O(4) | 89.15(14) |
| O(31)–Fe (1)–O(4) | 92.34(13) | O(10)–Fe(2)–O(4) | 90.53(12) |
| O(10)–Fe (1)–O(4) | 92.67(12) | O(11)–Fe(2)–N(19) | 88.41(14) |
| O(31)–Fe(1)–O(1) | 92.07(13) | O(10)–Fe(2)–N(19) | 172.28(15) |
| O(10)–Fe(1)–O(1) | 92.59(12) | O(4)–Fe (2)–N(19) | 86.90(13) |
| O(4)–Fe(1)–O(1) | 172.53(13) | O(11)–Fe(2)–N(22) | 166.50(14) |
| O(31)–Fe(1)–N(39) | 86.73(14) | O(10)–Fe(2)–N(22) | 93.55(14) |
| O(1)–Fe(1)–N(39) | 89.94(13) | O(4)–Fe(2)–N(22) | 85.35(15) |
| O(31)–Fe(1)–N(42) | 165.56(13) | N(19)–Fe(2)–N(22) | 79.00(15) |
| O(10)–Fe(1)–N(42) | 95.45(13) | O(11)–Fe(2)–Cl(1) | 95.29(11) |
| O(4)–Fe(1)–N(42) | 86.50(13) | O(10)–Fe(2)–Cl(1) | 93.29(9) |
| O(1)–Fe(1)–N(42) | 87.72(13) | O(4)–Fe(2)–Cl(1) | 173.63(10) |
| N(39)–Fe(1)–N(42) | 78.83(14) | N(19)–Fe(2)–Cl(1) | 88.66(11) |
| O(11)–Fe(2)–O(10) | 98.84(13) | N(22)–Fe (2)–Cl(1) | 89.32(12) |

The structure of **2** is also a dimer as shown in Figure 2. Here the two hexacoordinate iron atoms have different coordination spheres. Each is bound to the tridentate ligand and are bridged by hydroxide and formate ions. However, the coordination sphere of Fe(1) is completed by a monodentate formate ion and that of Fe(2) by a chloride ion. Complex **2** crystallizes in the monoclinic space group $P2_1/n$. The bridging hydroxide O(10) atom is 1.934(3) Å from Fe(1) and 1.926(3) Å from Fe(2) with an Fe(1)–O(10)–Fe(2) angle of 137.9(2)°. These dimensions are very different from those of the Fe–O–Fe bridge in **1a**. Indeed, the O(11), N(19), N(22), O(10) equatorial plane for Fe(2) and the O(31), N(39), N(42), O(10) equatorial plane for Fe(1) show root mean square deviations of 0.0257 and 0.0233 Å, respectively, with the metal atoms 0.066(2) and 0.025(2) Å from the planes. It is interesting to note that in **2**, the bridging hydroxido ligand completes an equatorial plane with the three donor atoms from L with both Fe(1) and Fe(2) in contrast with **1a**, where the bridging oxygen atom is in an axial position relative to L. Distances to L are equivalent for the two metal atoms. Thus, Fe(1)–O(31) 1.913(3) Å, Fe(1)–N(39) 2.116(4), and Fe(1)–N(42) 2.274(4) are equivalent to Fe(2)–O(11) 1.893(3) Å, Fe(2)–N(19) 2.100(4), and Fe(2)–N(22) 2.269(4) Å. The distances to the bridging formato ligand are, however, different due to the effect of the

  

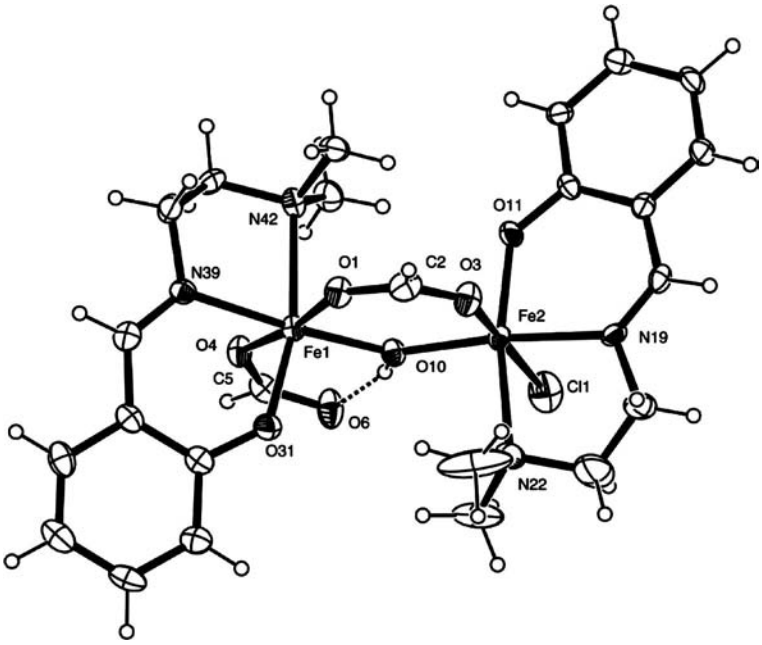


Figure 2. Structure of **2** with ellipsoids at 30% probability. The hydrogen bond is shown as a dotted line.

*trans* atoms with Fe(1)–O(1) 2.018(3) and Fe(2)–O(3) 2.081(3) Å. Further distances are to the monodentate formate Fe(1)–O(4) 2.013(3) Å and to the chloride ion Fe(2)–Cl(1) 2.368(2) Å. As shown in Figure 2, the bridging hydroxido O(10) forms a hydrogen bond to the unbound oxygen atom O(6) from the monodentate formate bound to Fe(1) with O(10)···O(6) 2.675(4) Å, O(10)–H(10)···O(6) 161°, and H(10)···O(6) 1.88 Å.

In this context we want to emphasize that most of the previously reported $Fe^{III}$ complexes of tridentate Schiff-base ligands are bis(Schiff base) complexes with noncoordinating counteranions such as $ClO_4^-$, $NO_3^-$, and $PF_6^-$.[16–18] Among the mono(Schiff base) complexes, alkoxido bridges (OMe, OEt) are found in three[19–21] and double phenoxido bridges in two.[19,22] The presence of a single μ-oxido bridge in **1a**, which contains a tridentate N,N,O donor Schiff-base ligand is uncommon, and, to the best of our knowledge, only one such example has been reported.[23] It is also worth mentioning that in all previously reported complexes of $Fe^{III}$ with this type of tridentate ligands, the $Fe^{III}$ ion is hexacoordinate, therefore the pentacoordinate $Fe^{III}$ observed in **1a** is unprecedented in such complexes.

## Theoretical Studies

As structures **1a** and **1b** exhibit very different Fe–O–Fe angles (142 and 166°, respectively), we have focused our theoretical study on providing a reasonable explanation for these values. We have performed theoretical calculations at the RI-BP86/def2-TZVP level of theory, which is a good compromise between the accuracy of the method and the size of the system. For the calculations, we have taken advantage of the $C_2$ symmetry of the structures observed in the solid state (see Figure 3).

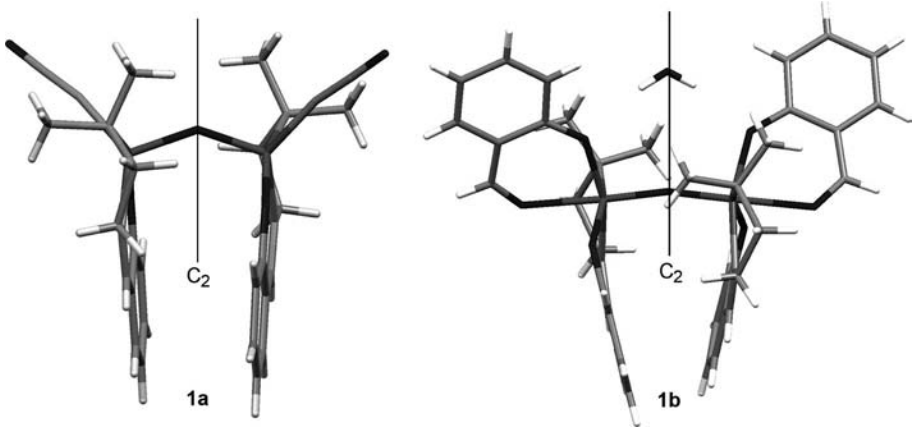


Figure 3. Representation of dimeric X-ray structures of compounds **1a** and **1b** including the $C_2$ symmetry axes.

  

Before analyzing the geometric and energetic features of compounds **1a** and **1b**, we have studied the range of Fe–O–Fe angles in the literature by analyzing the Cambridge Structural Database (CSD). Statistical analysis of structural data retrieved from the CSD provides a better understanding of the nature of a variety of covalent and noncovalent interactions and facilitates the identification of frequently occurring interaction patterns and supramolecular synthons. Therefore, we have performed a search in the CSD of compounds containing the μ-oxido bridge Fe–O–Fe imposing only one restriction: the absence of additional bidentate bridging ligands (acetate, phosphate etc.), which would obviously condition the Fe–O–Fe angle. By using the results of this search, a histogram of this angle has been generated, which is presented in Figure 4. It is very clear that the preference for this angle is 180°, and this preference does not depend upon the coordination number of the Fe ion.

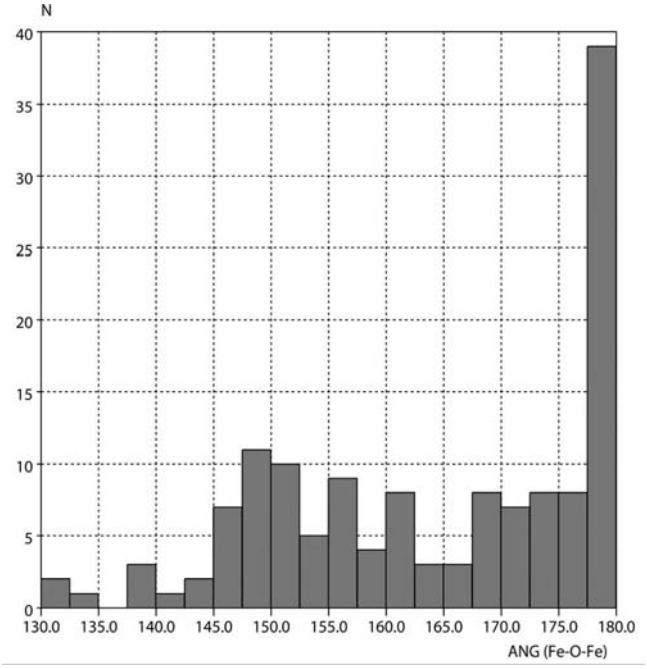


Figure 4. Histogram of the Fe–O–Fe angles [°] obtained from the CSD in dinuclear $Fe^{III}$ compounds.

Curiously, **1a** has an Fe–O–Fe angle of 142°, which is considerably smaller than that found in the majority of hits. In fact, only seven X-ray structures have angles lower than 142.5°. Our theoretical study is focused on explaining the very small angle observed for the μ-oxido bridge in **1a** and for that observed in **1b**, which is due to the presence of a water molecule. It is clear that in **1b**, the geometry of the dimer is not due to the covalency of the metal–ligand bonds, but rather to noncovalent interactions that are considerably weaker.

### Theoretical Study of 1a

Calculations on **1a** have been divided into two parts: the first is devoted to the study of how the energy changes as a function of the μ-oxido bridge angle. In Table 2 we summarize the relative energy of **1a** imposing several values for the Fe–O–Fe angle in the calculations. The variation in energy is represented in Figure 5. It can be observed that the relative energy becomes more positive as the angle increases, indicating that in **1a** the most stable geometry does not correspond to an angle of 180°, as is common in this type of compound, see Figure 4. It can be observed that the structure corresponding to an Fe–O–Fe angle of 180° is just a local minimum. We have also computed the energy of the system at 140°, see Table 2, and the energy drastically increases by 0.87 kcal/mol. We have examined the geometry of **1a** at the minimum and an unconventional π–π interaction between both aromatic ligands is observed (Figure 6). That is, the aromatic rings themselves are not stacked; however, since the π-system is extended to the imidic C=N bond by conjugation, two C–C bonds with partial double-bond character are stacked. The distance between the middle of both C–C bonds is 3.3 Å, characteristic of π–π interactions.[28] We have performed the "atoms-in-molecules" (AIM) analysis of **1a** to confirm this feature. The AIM analysis, by means of the distribution of critical points, gives an unambiguous confirmation of the presence of an interaction.[29] The AIM analysis shows a bond critical point that connects one aromatic carbon atom of one ring with another aromatic carbon of the other ring, confirming the interaction (Figure 7). The value of the density at the bond critical point is $10^2 \times \rho = 0.547$ a.u., which is of the same magnitude as standard π–π interactions.[30] The presence of this weak interaction explains the small Fe–O–Fe angle observed in the solid-state structure of **1a** as the energy at 180° is only 0.86 kcal/mol more positive than that

Table 2. Relative energies [kcal/mol] of different conformers of **1a** at the RI-PB86/def2-TZVP level of theory.

| Fe–O–Fe [°] | $E_{rel}$ [kcal/mol] |
|---|---|
| 140 | 0.87 |
| 142 | 0.00 |
| 145 | 0.64 |
| 150 | 1.00 |
| 160 | 1.07 |
| 170 | 1.09 |
| 175 | 0.99 |
| 180 | 0.86 |

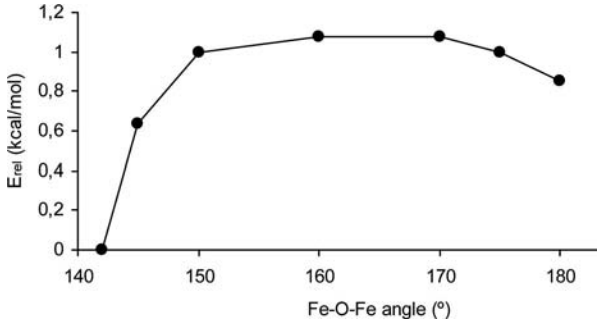


Figure 5. Graphical representation of the relative energy ($E_{rel}$) vs. the Fe–O–Fe angle in °.

  

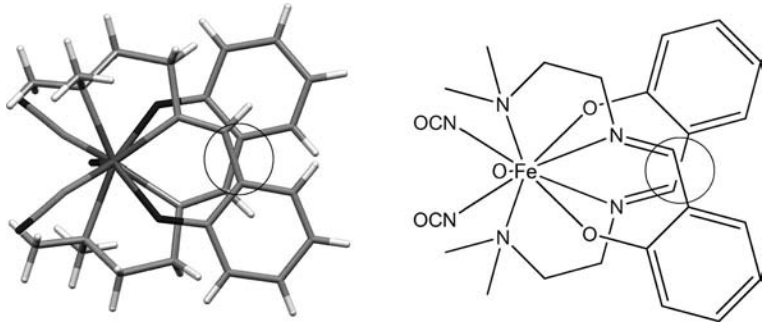


Figure 6. Representation of the structure of **1a** with indication of the stacked C–C bonds.

at 142°. This result agrees with the fact that "state of the art" calculations on the π–π stacking of the benzene dimer predicts an interaction energy of –1 kcal/mol,[31] which is similar to the energetic difference between both geometries (142° and 180°) of 0.86 kcal/mol.

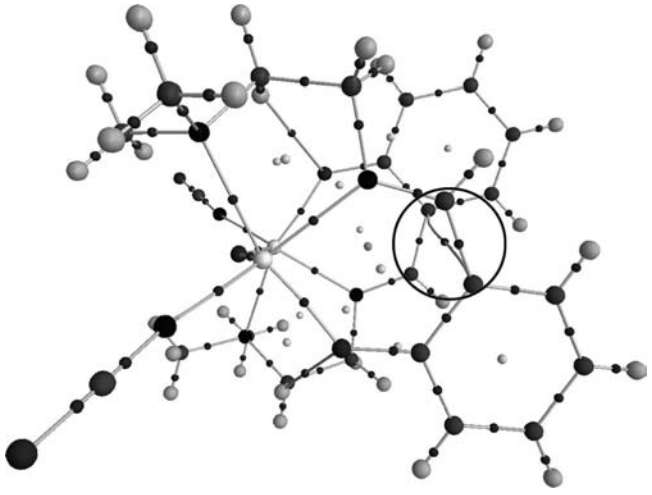

Figure 7. Distribution of critical points in **1a**. The bond critical point (black small sphere) and bond path that characterizes the π–π interaction is marked by a black circle. Ring critical points are indicated by small light grey spheres.

### Theoretical Study of 1b

In the structure of **1b** the Fe–O–Fe angle is clearly influenced by the presence of a water molecule in the crystal structure interacting with the phenolic oxygen atoms (see Figure 8). We have performed two types of calculation on this structure. First, we studied the influence of the Fe–O–Fe angle on the relative energy of **1b** in the absence and presence of a water molecule. Secondly, we computed the interaction energy between a water molecule and the dinuclear structure of **1b** at the minimum.

In Table 3 we summarize the relative energy of **1b** at different Fe–O–Fe angles. It is interesting to note that the calculation with a water molecule indicates that the minimum is located at 166°, as observed in the crystal structure. In contrast when the water molecule is eliminated and the energy profile is computed, the minimum is found at 180°, as expected. Therefore, the formation of the hydrogen bonds compensates for the energy difference between 180° and 166°, which is –1.49 kcal/mol. This explanation has been confirmed by the calculation of the interaction energy between the complex and a water molecule, which is –11.8 kcal/mol. Therefore, the presence of a water molecule in this compound is crucial to explain the experimental Fe–O–Fe angle. It is clear from the energy profile of this complex in the absence of a water molecule that the flexibility of the Fe–O–Fe motif allows the complex to adopt the energetically most favorable conformation by maximizing noncovalent attractive interactions.

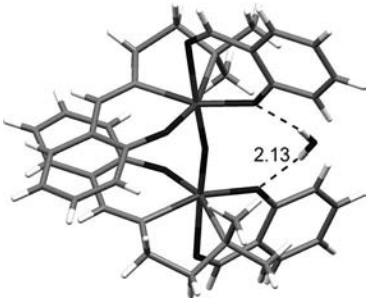


Figure 8. Hydrogen bonds between a water molecule and the phenolic oxygen atoms. Distance in Å as found in the crystal structure.

Table 3. Relative energies [kcal/mol] of **1b** with ($E_{rel\_w}$) and without ($E_{rel}$) the water molecule.

| Fe–O–Fe [°] | $E_{rel\_w}$ [kcal/mol] | $E_{rel}$ [kcal/mol] |
|---|---|---|
| 160 | 8.62 | 7.16 |
| 165 | 2.09 | 0.92 |
| 166 | 0.00 | 0.00 |
| 170 | 0.01 | –1.11 |
| 180 | 1.07 | –1.49 |

## Conclusions

We have synthesized two new nonheme diiron(III) complexes with a tridentate N,N,O donor Schiff-base ligand (**1a** and **2**), and we have characterized them experimentally by

  

elucidating their crystal structures. In addition, we have carried out calculations on structures **1a** and **1b** at the RI-BP86/def2-TZVP level of theory in order to study the influence of noncovalent interactions on the Fe–O–Fe angle. To accomplish this, we have computed the energy profiles of both compounds depending on the μ-oxido bridge angle. Intra- (**1a**) or internoncovalent (**1b**) interactions are responsible for the observed differences in the values of the Fe–O–Fe angle. A CSD search indicates that 180° is the most abundant situation; however, the energy cost of bending is not high, and, consequently, it is easily compensated for by other forces that may exist in the crystal structure.

## Experimental Section

**Starting Materials:** Salicylaldehyde, *N*,*N*-dimethylethane-1,2-diamine, sodium cyanate, and sodium formate were purchased from commercial sources and used as received. Solvents were of reagent grade and were used without further purification.

**Physical Measurements:** Elemental analyses (C, H, and N) were performed with a Perkin–Elmer 240C elemental analyzer. IR spectra as KBr pellets (4500–500 $cm^{-1}$) were recorded with a Perkin–Elmer RXI FTIR spectrometer. Electronic spectra (1000–200 nm) were recorded with a Hitachi U-3501 spectrophotometer. The electronic absorption spectra of complexes **1b** and **2** were measured in $CH_3OH$ and that of **1a** in $CH_3CN$ due to its low solubility in methanol.

**Theoretical Methods:** The geometries of all complexes studied in this work were computed at the RI-BP86/def2-TZVP level of theory with TURBOMOLE version 5.7 using the crystallographic coordinates.[32] We have used the BP86 method[33] and the def2-TZVP,[34] basis set because this level of theory has been successfully used by our group[35] and others[36] to study organometallic complexes theoretically. The RI-DFT method applied to the study of weak interactions is considerably faster than DFT, and the interaction energies and equilibrium distances are almost identical for both methods.[37] In addition the RI approximation is very efficient provided that the functional is of nonhybrid type.[32] We have considered high-spin density for the $Fe^{III}$ atoms in the calculations. The AIM analysis[38,29] of the complexes was performed with the AIM2000 version 2.0 program[39] by using the BP86/def2-TZVP wavefunction and the geometry obtained from the crystallographic coordinates.

**Synthesis of 2-({[2-(Dimethylamino)ethyl]imino}methyl)phenol (HL):** Salicylaldehyde (1.05 mL, 10 mmol) and *N*,*N*-dimethylethane-1,2-diamine (1.098 mL, 10 mmol) in methanol (10 mL) were heated under reflux for 1 h. The Schiff-base ligand was not isolated, and the yellow methanolic solution was used directly for complex formation.

**Synthesis of 1a:** A methanolic solution (10 mL) of L (5 mmol) was added to a methanolic solution of $FeCl_3$ (0.811 g, 5 mmol) with constant stirring. After ca. 15 min, a methanolic solution of sodium cyanate (0.650 g, 10 mmol) was added, and the color of the solution turned to dark-red immediately. The solution was left to stand in air until dark-red X-ray quality single crystals of **1a** appeared at the bottom of the vessel after slow evaporation of the solvent. Yield 1.11 g (75%). $C_{24}H_{30}Fe_2N_6O_5$ (594.24): calcd. C 48.51, H 5.09, N 14.14; found C 48.47, H 5.01, N 14.10. IR (KBr pellet): $\tilde{\nu}$ = 1614.7, 2205 $cm^{-1}$. UV/Vis ($CH_2Cl_2$): $\lambda$ ($\varepsilon$) = 415 (4800), 493 (2700), 317 (17000), 255 (38000), 231 (59000 $dm^3\,mol^{-1}\,cm^{-1}$) nm.

**Synthesis of 1b:** A methanolic solution (10 mL) of L (5 mmol) was added to a methanolic solution of $FeCl_3$ (0.811 g, 5 mmol) with constant stirring. Triethylamine (0.21 mL, 2.5 mmol) was added dropwise to the solution with constant stirring. The color of the solution turned to dark-red immediately. The solution was left to stand in air until dark-red X-ray quality single crystals of **1b** appeared at the bottom of the vessel after slow evaporation of the solvent. Yield 0.62 g (33%, with respect to Fe). $C_{36}H_{42}Fe_2N_4O_8$ (752.438): calcd. C 56.12, H 5.49, N 7.27; found C 56.01, H 5.40, N 7.17. IR (KBr pellet): $\tilde{\nu}$ = 1617.6 $cm^{-1}$. UV/Vis ($CH_3OH$): $\lambda$ ($\varepsilon$) = 427 (2400), 509 (2450), 318 (6000), 260 (11900), 233 (21400 $dm^3\,mol^{-1}\,cm^{-1}$) nm.

**Synthesis of 2:** A methanolic solution (10 mL) of L (5 mmol) was added to a methanolic solution of $FeCl_3$ (0.811 g, 5 mmol) with constant stirring. After ca. 15 min, a methanolic solution of sodium formate (0.680 g, 10 mmol) was added, and the color of the solution turned to dark-red immediately. The solution was left to stand in air until dark-red X-ray quality single crystals of **2** appeared at the bottom of the vessel after slow evaporation of the solvent. Yield 1.08 g (68%). $C_{24}H_{33}ClFe_2N_4O_7$ (635.69): calcd. C 45.27, H 5.22, N 8.80; found C 45.18, H 5.10, N 8.72. IR (KBr pellet): $\tilde{\nu}$ = 1632.1, 1581.4, 3431.4 $cm^{-1}$. UV/Vis ($CH_3OH$): $\lambda$ ($\varepsilon$) = 411 (6800), 510 (1600), 320 (32000), 256 (70500), 234 (90400 $dm^3\,mol^{-1}\,cm^{-1}$) nm.

**Crystal Data Collection and Refinement:** The independent number of reflections for **1a**, **1b**, and **2** are 2206, 4990, and 7603, respectively. They were collected with Mo-$K_\alpha$ radiation at 150 K by using an Oxford Diffraction X-Calibur CCD System. The crystals were positioned at 50 mm from the CCD. The number of frames measured was 321 with a counting time of 10 s. Data analyses were carried out with the CrysAlis program.[40] The structures were solved by direct methods with the SHELXS97 program.[41] The non-hydrogen atoms were refined with anisotropic thermal parameters. The hydrogen atoms bound to carbon atoms were included in geometric positions and given thermal parameters equivalent to 1.2 (or 1.5 for methyl groups) times those of the atom to which they were attached. Hydrogen atoms of the water molecule in **1b** were located in a difference Fourier map and refined with distance constraints. Absorption corrections were carried out by using the ABSPACK program.[42] The structures were refined on $F^2$ to $R_1$ =

Table 4. Crystal data and structure refinement of complexes **1a** and **2**.

| | **1a** | **2** |
|---|---|---|
| Empirical formula | $C_{24}H_{30}Fe_2N_6O_5$ | $C_{24}H_{32}ClFe_2N_4O_7$ |
| $M$ | 594.24 | 635.69 |
| Crystal system | orthorhombic | monoclinic |
| Space group | $Fdd2$ | $P2_1/n$ |
| $a$ [Å] | 31.0762(8) | 12.9340(7) |
| $b$ [Å] | 17.4559(16) | 12.5115(6) |
| $c$ [Å] | 9.731(2) | 17.1490(11) |
| $\beta$ [°] | 90 | 97.905(5) |
| $V$ [Å$^3$] | 5278.5(12) | 2748.8(3) |
| $Z$ | 8 | 4 |
| $D_{calcd.}$ [g cm$^{-3}$] | 1.495 | 1.536 |
| $\mu$ [mm$^{-1}$] | 1.145 | 1.202 |
| $F$(000) | 2464 | 1316 |
| $R$(int) | 0.063 | 0.089 |
| Total reflections | 4625 | 16622 |
| Unique reflections | 2206 | 7603 |
| $I > 2\sigma(I)$ | 1370 | 2679 |
| $R_1$, $wR2$ | 0.0354, 0.0594 | 0.0574, 0.1235 |
| $T$ [K] | 150 | 150 |

  

0.0354, 0.0452, 0.0574; $wR_2$ = 0.0594, 0.0745, 0.1048 for 1370, 2724, 2679 data with $I > 2\sigma(I)$. Details of crystallographic data and refinements are summarized in Table 4. The refinement and structural parameters of **1b** are very similar to those of the reported complex.[23] Therefore, we do not include the crystallographic information for this compound. CCDC-806718 (for **1a**), -806719 (for **1b**) and -806720 (for **2**) contain the supplementary crystallographic data for this paper. These data can be obtained free of charge from The Cambridge Crystallographic Data Centre via www.ccdc.cam.ac.uk/data_request/cif.

**Supporting Information** (see footnote on the first page of this article): Infrared and electronic absorption spectra of the complexes **1a**, **1b**, and **2**.

## Acknowledgments

R. B. is thankful to the Council of Scientific and Industrial Research (CSIR), India, for a research fellowship [Sanction no.09/028 (0746)/2009-EMR-I]. We thank the British Engineering and Physical Sciences Research Council (EPSRC) and the University of Reading for funds for the X-Calibur system. C. E. thanks the Ministerio de Educación y Ciencia (MEC) of Spain for a predoctoral fellowship. We thank the CONSOLIDER-Ingenio 2010 (CSD2010-00065) and the Ministerio de Ciencia e Innovación (MICINN) of Spain (Project CTQ2008-00841/BQU) for financial support.

[1] a) H. Zheng, Y. Zang, Y. Dong, V. G. Young, L. Que, *J. Am. Chem. Soc.* **1999**, *121*, 2226–2235; b) I. M. Wasser, C. F. Martens, C. N. Verani, E. Rentschler, H.-W. Huang, P. M. Moenne-Loccoz, L. N. Zakharov, A. L. Rheingold, K. D. Karlin, *Inorg. Chem.* **2004**, *43*, 651–662; c) J. B. Vincent, G. L. Olivier-Lilley, B. A. Averill, *Chem. Rev.* **1990**, *90*, 1447–1467; d) G. Haselhorst, K. Wieghardt, S. Keller, B. Schrader, *Inorg. Chem.* **1993**, *32*, 520–525.

[2] a) A. B. Hoffman, D. M. Collins, V. W. Day, E. B. Fleischer, T. S. Srivastava, J. L. Hoard, *J. Am. Chem. Soc.* **1972**, *94*, 3620–3626; b) J. T. Landrum, D. Grimmett, K. J. Haller, R. W. Scheidt, C. A. Reed, *J. Am. Chem. Soc.* **1981**, *103*, 2640–2650.

[3] a) R. N. Mukherjee, T. D. P. Stack, R. H. Holm, *J. Am. Chem. Soc.* **1988**, *110*, 1850–1861; b) S. Koner, S. Iijima, M. Watanabe, M. Sato, *J. Coord. Chem.* **2003**, *56*, 103–111; c) F. Corazza, C. Floriani, M. Zehnder, *J. Chem. Soc., Dalton Trans.* **1987**, 709–714.

[4] S. K. Ghosh, R. Patra, S. P. Rath, *Inorg. Chem.* **2010**, *49*, 3449–3460.

[5] S. K. Ghosh, R. Patra, S. P. Rath, *Inorg. Chim. Acta* **2010**, *363*, 2791–2799.

[6] a) W. R. Scheidt, B. Cheng, M. K. Safo, F. Cukiernik, J. C. Marchon, P. G. Debrunner, *J. Am. Chem. Soc.* **1992**, *114*, 4420–4421; b) B. Cheng, J. Hobbs, D. P. G. Debrunner, J. Erlebacher, J. A. Shelnutt, W. R. Scheidt, *Inorg. Chem.* **1995**, *34*, 102–110.

[7] K. M. Kadish, M. Antret, Z. O. Tagliatesta, P. T. Soschi, V. Fares, *Inorg. Chem.* **1997**, *36*, 204–207.

[8] D. R. Evans, R. S. Mathur, K. Heerwegh, C. A. Reed, Z. Xie, *Angew. Chem. Int. Ed. Engl.* **1997**, *36*, 1335–1337.

[9] Z.-L. You, L.-L. Tang, H.-L. Zhu, *Acta Crystallogr., Sect. E* **2005**, *61*, m36–m38.

[10] D. J. Darensbourg, C. G. Ortiz, D. R. Billodeaux, *Inorg. Chim. Acta* **2004**, *357*, 2143–2149.

[11] a) E. C. Wilkinson, Y. Dong, L. Que, *J. Am. Chem. Soc.* **1994**, *116*, 8394–8395; b) A. B. Ozarowski, R. McGarvey, J. E. Drake, *Inorg. Chem.* **1995**, *34*, 5558–5566; c) L. Vernik, D. V. Stynes, *Inorg. Chem.* **1996**, *35*, 2006–2010; d) J. Wang, M. S. Mashuta, Z. Sun, J. F. Richarson, D. N. Hendrickson, R. M. Buchanan, *Inorg. Chem.* **1996**, *35*, 6642–6643; e) C. Duboc-Toia, S. Ménage, J.-M. Vincent, M. T. Averbuch-Pouchot, M. Fontecave, *Inorg. Chem.* **1997**, *36*, 6148–6149; f) F. Calderazzo, F. Marchetti, *J. Chem. Soc., Dalton Trans.* **1998**, 1485–1490.

[12] J. Jullien, G. Juhász, P. Mialane, E. Dumas, C. R. Mayer, J. Marrot, E. Rivière, E. L. Bominaar, E. Münck, F. Sécheresse, *Inorg. Chem.* **2006**, *45*, 6922–6927.

[13] X. Wang, S. Wang, L. Li, E. B. Sundberg, G. P. Gacho, *Inorg. Chem.* **2003**, *42*, 7799–7808.

[14] A.-R. Li, H.-H. Wei, L.-L. Gang, *Inorg. Chim. Acta* **1999**, *290*, 51–56.

[15] a) B. Sarkar, M. Sinha Ray, Y.-Z. Li, Y. Song, A. Figuerola, E. Ruiz, J. Cirera, J. Cano, A. Ghosh, *Chem. Eur. J.* **2007**, *13*, 9297–9309; b) C. Biswas, M. G. B. Drew, E. Ruiz, M. Estrader, C. Diaz, A. Ghosh, *Dalton Trans.* **2010**, *39*, 7474–7484; c) P. Mukherjee, M. G. B. Drew, C. J. Gomez-García, A. Ghosh, *Inorg. Chem.* **2009**, *48*, 5848–5860; d) P. Mukherjee, M. G. B. Drew, M. Estrader, A. Ghosh, *Inorg. Chem.* **2008**, *47*, 7784–7791; e) C. Biswas, M. G. B. Drew, A. Ghosh, *Inorg. Chem.* **2008**, *47*, 4513–4519.

[16] M. D. Timken, D. N. Hendrickson, E. Sinn, *Inorg. Chem.* **1985**, *24*, 3947–3955.

[17] P. G. Sim, E. Sinn, R. H. Petty, C. L. Merrill, L. J. Wilson, *Inorg. Chem.* **1981**, *20*, 1213–1222.

[18] S. Hayami, S. Miyazaki, M. Yamamoto, K. Hiki, N. Motokawa, A. Shuto, K. Inoue, T. Shinmyozu, Y. Maeda, *Bull. Chem. Soc. Jpn.* **2006**, *79*, 442–450.

[19] F. Banse, V. Balland, C. Philouze, E. Riviere, L. Tchertanova, J.-J. Girerd, *Inorg. Chim. Acta* **2003**, *353*, 223–230.

[20] B. Chiari, O. Piovesana, T. Tarantelli, P. F. Zanazzi, *Inorg. Chem.* **1984**, *23*, 3398–3404.

[21] B. Chiari, O. Piovesana, T. Tarantelli, P. F. Zanazzi, *Inorg. Chem.* **1982**, *21*, 1396–1402.

[22] Z.-L. You, H.-L. Zhu, *Acta Crystallogr., Sect. E: Struct. Rep. Online* **2004**, *60*, m1046–m1048.

[23] G. Das, R. Shukla, S. Mandal, R. Singh, P. K. Bharadwaj, *Inorg. Chem.* **1997**, *36*, 323–329.

[24] C. Ercolani, M. Gardini, F. Monacelli, G. Pennesi, G. Rossi, *Inorg. Chem.* **1983**, *22*, 2584–2589.

[25] a) R. C. Reem, J. M. McCormick, D. E. Richardson, F. J. Devlin, P. J. Stephens, R. L. Musselman, E. I. Solomon, *J. Am. Chem. Soc.* **1989**, *111*, 4688–4704; b) S. J. Lippard, H. J. Schugar, C. Walling, *Inorg. Chem.* **1967**, *6*, 1825–1831; c) H. J. Schugar, G. R. Rossman, C. G. Barraclough, H. B. Gray, *J. Am. Chem. Soc.* **1972**, *94*, 2683–2690.

[26] a) Y.-G. Wei, S.-W. Zhang, M.-C. Shao, *Polyhedron* **1997**, *16*, 2307–2313; b) S. L. Heath, A. K. Powell, H. L. Utting, M. Helliwell, *J. Chem. Soc., Dalton Trans.* **1992**, 305–307 and references cited therein .

[27] T. Dahl, *Acta Chem. Scand.* **1994**, *48*, 95–106.

[28] C. A. Hunter, J. K. M. Sanders, *J. Am. Chem. Soc.* **1990**, *112*, 5525–5534.

[29] R. F. W. Bader, *Chem. Rev.* **1991**, *91*, 893–928.

[30] D. Quiñonero, A. Frontera, C. Garau, P. Ballester, A. Costa, P. M. Deyà, *ChemPhysChem* **2006**, *7*, 2487–2491.

[31] S. K. Min, E. C. Lee, D. Y. Kim, D. Kim, K. S. Kim, *J. Comput. Chem.* **2008**, *29*, 1208–1221.

[32] R. Ahlrichs, M. Bär, M. Häser, H. Horn, C. Kölmel, *Chem. Phys. Lett.* **1989**, *162*, 165–169.

[33] a) A. D. Becke, *Phys. Rev. A* **1988**, *38*, 3098–3100; b) J. P. Perdew, *Phys. Rev. B* **1986**, *33*, 8822–8824.

[34] F. Weigend, R. Ahlrichs, *Phys. Chem. Chem. Phys.* **2005**, *7*, 3297–3305.

[35] a) S. Naiya, M. G. B. Drew, C. Estarellas, A. Frontera, A. Ghosh, *Inorg. Chim. Acta* **2010**, *363*, 3904–3913; b) S. Biswas, S. Naiya, M. G. B. Drew, C. Estarellas, A. Frontera, A. Ghosh, *Inorg. Chim. Acta* **2010**, *366*, 219–226.

[36] a) R. D. Dewhurst, R. Müller, M. Kaupp, K. Radacki, K. Götz, *Organometallics* **2010**, *29*, 4431–4433; b) A. Anoop, W.

  

Thiel, F. Neese, *J. Chem. Theory Comput.* **2010**, *6*, 3137–3144.
[37] D. Quiñonero, C. Garau, A. Frontera, P. Ballester, A. Costa, P. M. Deyà, *J. Phys. Chem. A* **2006**, *110*, 5144–5157.
[38] R. F. W. Bader, *Atoms in Molecules – A Quantum Theory*, Clarendon, Oxford, U. K., **1990**.
[39] F. Biegler-König, J. Schönbohm, D. Bayles, *J. Comput. Chem.* **2001**, *22*, 545–559.
[40] *CrysAlis*, Oxford Diffraction Ltd., Abingdon, U. K., **2006**.
[41] SHELXS97 and SHELXL97, Programs for Crystallographic solution and refinement: G. M. Sheldrick, *Acta Crystallogr., Sect. A* **2008**, *64*, 112–122.
[42] *ABSPACK*, Oxford Diffraction Ltd., Oxford, U. K., **2005**.
Received: January 11, 2011
Published Online: April 18, 2011

  